ISSN 1070-3632, Russian Journal of General Chemistry, 2016, Vol. 86, No. 11, pp. 2508–2514. © Pleiades Publishing, Ltd., 2016.
Original Russian Text © E.A. Katlenok, A.A. Zolotarev, K.P. Balashev, 2016, published in Zhurnal Obshchei Khimii, 2016, Vol. 86, No. 11, pp. 1866–1872.

Influence of Ligand Donor-Acceptor Properties on the Structure, Optical, and Electrochemical Characteristics of Ir(III) Complexes with Cyclometallated 2-Phenylbenzotiazole

E. A. Katlenok[a], A. A. Zolotarev[b], and K. P. Balashev[a]*

[a] *Herzen State Pedagogical University of Russia, nab. reki Moiki 48, St. Petersburg, 191186 Russia*
**e-mail: k_balashev@mail.ru*

[b] *St. Petersburg State University, St. Petersburg, Russia*

Received May 10, 2016

Abstract—The *cis*-C,C-structure of a series of cyclometallated Ir(III) complexes with 2-phenylbenzotiazole was determined by the methods of X-ray diffraction (XRD) analysis, ^{1}H, ^{13}C, ^{31}P NMR, and IR spectroscopy. Long-wave absorption bands, phosphorescence, and processes of electrochemical oxidation and reduction of the complexes were assigned to the transfer of electrons presumably located on d_{π} and π^* orbitals of cyclometallated 2-phenylbenzotiazole. The decrease in donor and acceptor properties of the ligands leads to the blue shift of absorption spectra and phosphorescence and to the anodic shift of oxidation and reduction potentials of the complexes.

Keywords: cyclometallated Ir(III) complexes, molecular structure, X-ray diffraction analysis, ^{1}H, ^{13}C, ^{31}P NMR, optical and electrochemical characteristics

DOI: 10.1134/S1070363216110177

Phosphorescence at room temperature and reversibility of electrochemical processes of outer-sphere electron transfer of Ir(III) cyclometallated complexes define wide prospects for their use in organic light-emitting diodes [1], photocatalysts [2], fluorescent markers of biosystems [3], and chemosensors [4]. The nature of a cyclometallated ligand affects the optical and electrochemical characteristics of complexes, causing their variation in wide intervals. The presence of chelating ligands with variable donor-acceptor properties in mixed-ligand biscyclometallated complexes allows changing their optical and electrochemical properties by variation of the energies of the highest occupied and the lowest unoccupied molecular orbitals (HOMO and LUMO).

We have studied the structure and optical and electrochemical properties of the complexes $[Ir(bt)_2(t\text{-BuNC})_2]\cdot$

Scheme 1.

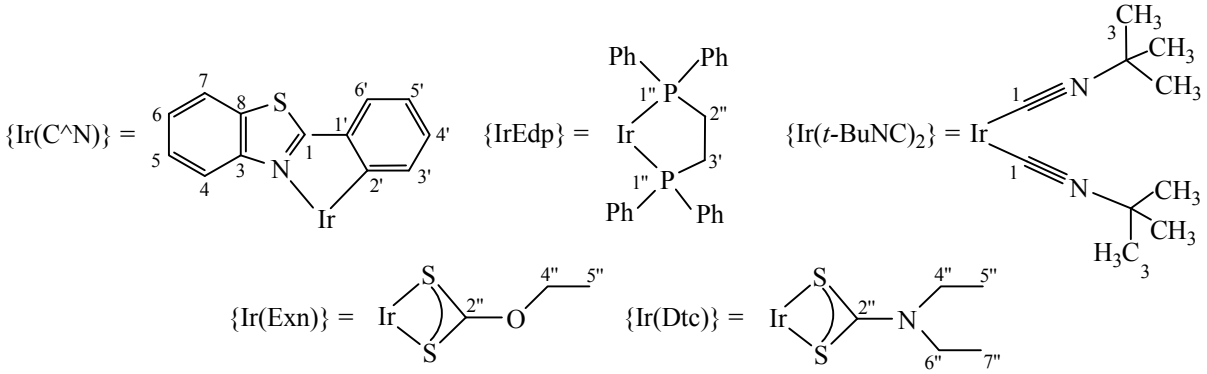

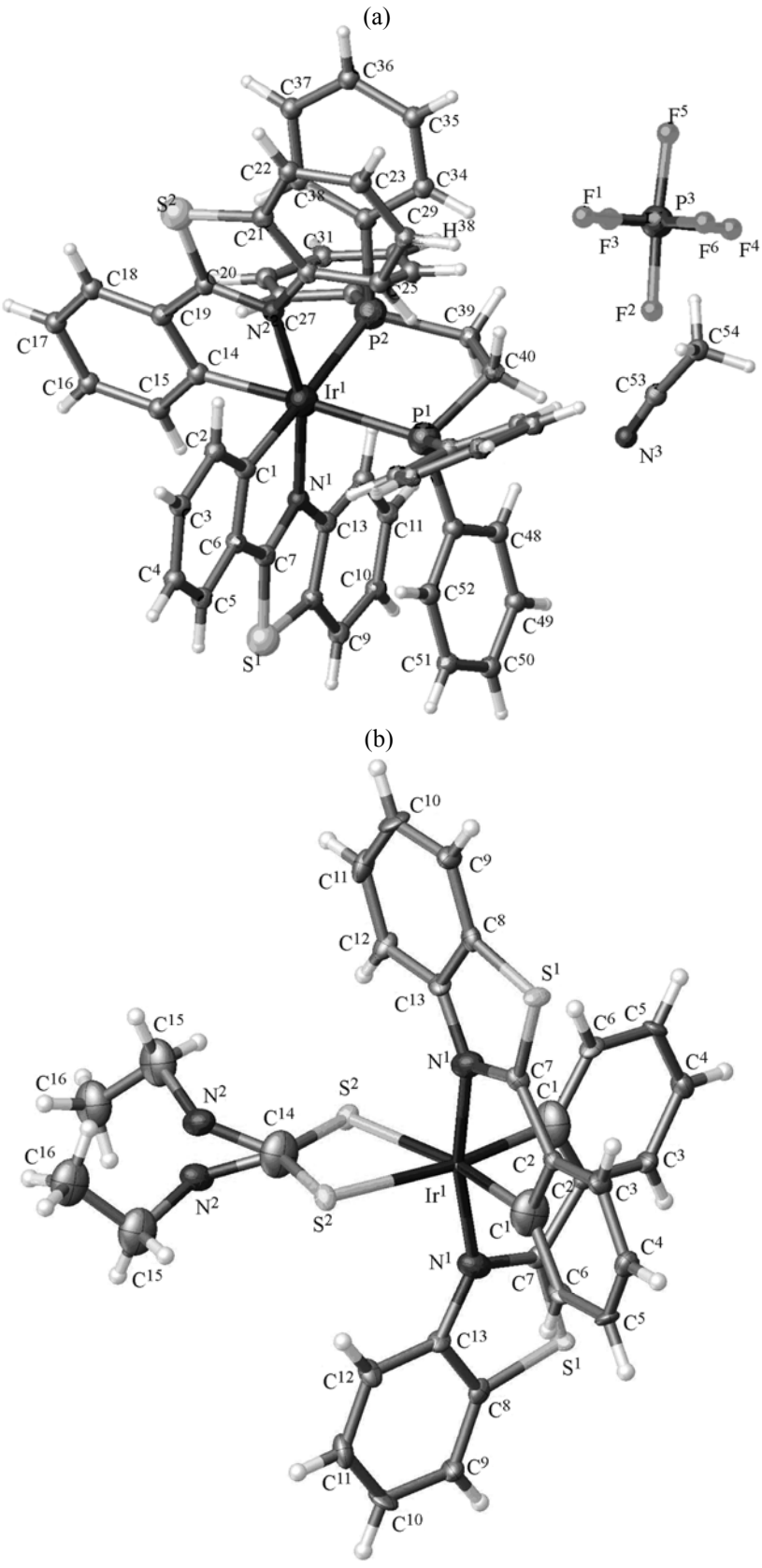

Fig. 1. Molecular structure of complexes (a) $[Ir(bt)_2Edp]PF_6 \cdot CH_3CN$ and (b) $[Ir(bt)_2Dtc]$ in the unit cell.

Table 1. Crystallographic and refining structural parameters of complexes **2** and **4**

Complex	$[Ir(bt)_2Edp]PF_6 \cdot CH_3CN$	$[Ir(bt)_2Dtc]$
Empirical formula	$C_{54}H_{43}F_6IrN_3P_3S_2$	$C_{16}H_{13}PtNOS_3$
M	1197.14	526.54
Crystal system	Monoclinic	Monoclinic
Space group	$P2_1/n$	$P2_1/c$
a, Å	17.4559(3)	10.0437(3)
b, Å	14.7400(3)	5.68736(17)
c, Å	18.7150(3)	27.6934(9)
β, deg	97.8460(16)	90.070(3)
V, Å^{-3}	4770.29(15)	1581.91(8)
Z	4	4
d_{calc}, g/cm^3	1.667	2.211
μ, mm^{-1}	7.745	9.265
F(000)	2384.0	1000.0
2θ Range, deg	6.496–144.982	7.144–56.00
Radiation	CuK_α	MoK_α
Index range	$-21 \le h \le 17$, $-18 \le k \le 18$, $-23 \le l \le 23$	$-13 \le h \le 11$, $-4 \le k \le 7$, $-28 \le l \le 36$
Total of reflexes	25616	9115
Independent reflexes (R_{int})	9267 (R_{int} = 0.0391)	3788 (R_{int} = 0.0578)
GoF	1.052	1.026
R-Factors ($F_0 \ge 4\sigma_F$)	R_1 = 0.0337, wR_2 = 0.0756	R_1 = 0.0477, wR_2 = 0.1217
ρ_{min}, ρ_{max}, e/Å^{-3}	1.36/–0.91	4.53/–3.19

PF_6 (**1**), $[Ir(bt)_2(Edp)]PF_6$ (**2**), $[Ir(bt)_2(Exn)]$ (**3**), and $[Ir(bt)_2(Dtc)]$ (**4**), in which cyclometallated 2-phenylbenzotiazole [Ir(bt)] is bound with π-acceptor [*tert*-butylisocianide (*t*-BuNC), 1,2-bis(diphenylphosphinio) ethane (Edp)], and π-donor [ethylxanthogenate (Exn) and diethyldithiocarbamate (Dtc^-)] ligands (Scheme 1).

The XCA data of complexes **2** and **4** (Fig. 1, Table 1) show that they have distorted octahedral structure with the typical [5–8] *cis*-C,C position of two cyclometallated ligands and the *trans*-position of donor S and P atoms of chelating ligands in relation to C atoms. It leads to the equivalence of Ir-S bonds in the four-membered chelate cycle {IrDtc} and a minor difference (Δr = 0.004 Å) between Ir–P bonds in the five-membered cycle {IrEdp}. The *cis*-position of S and N donor atoms of chelating and cyclometallated ligands leads to the formation of intramolecular hydrogen bonds between S and H[4] atoms in complex **4** [3.943(3) Å].

The sum of Ir(III) bond angles involving donor C atoms of 2-phenylbenzothiazole ligands and P or S atoms of chelating ligands (Table 2) is almost equal to 360° that corresponds to the presence of the Ir(III) atom in the plane of these donor atoms. Deviations by 10.5° and 12.8° of donor atoms N of benzothiazole components of metallated ligands from the perpendicular position to the equatorial plane of the complexes **1** and **2** result in the distortion of their octahedral structures. The length of the Ir–N(bt) bond and the bond angle C(bt)IrN(bt) of complexes **2** and **4** (Table 3) are the same as for the complexes with other chelating ligands [5–8]. The π–acceptor interaction of 1.2-bis(diphenylphosphino)ethane with the metal in complex **2** results in the elongation of the Ir–C(bt)

bond by 0.075 Å as compared with complex **4**. The formation of the {IrDtc} chelate cycle is accompanied by the increase in multiplicity of the C–N bond and the decrease in its length by ~0.1 Å. A similar decrease in the length of C–N bond as a result of the increase in its multiplicity was previously noted [9] for the cyclometallated complex [Pt(bzq)Dmtc] (bzq$^-$ and Dmtc$^-$ are deprotonated forms of benzo[*h*]quinoline and dimethyldithiocarbamate).

The IR spectroscopy data confirm the ligand coordination in complexes **1**–**4** and point to the presence of the outer-sphere ion PF_6^- with characteristic frequency 841 cm^{-1} of P–F stretching vibrations [10] in complexes **1** and **2**. Frequencies of SCS vibrations in the spectra of complexes **3** and **4** (Table 4) confirm the bidentate coordinated of the Dtc$^-$ and Exn$^-$ ligands [11]. The increase in the frequency of stretching C–N and C–O vibrations of coordinated Dtc$^-$ and Exn$^-$ ions by 11 and 34 cm^{-1} as compared to sodium salts of diethyldithiocarbamate and ethylxanthogenate is consistent with the increase in multiplicity of C–N and C–O bonds. Coordination of π-acceptor *t*-BuNC leads to the increase in the C=N vibration by 34 and 63 cm^{-1} as compared to the free ligand.

The ^{1}H NMR spectroscopy data for the complexes point to the retention of their *cis*-C,C structure in solution, as evidenced by the magnetic equivalence of two cyclometallated ligands and by mutual anisotropic action of circular currents of their phenyl components, which result (Table 3) in the upfield shift of H^3 signals by 0.7–0.8 ppm in the complex as compared with free 2-phenylbenzotiazole. Close (~3 Å) positions of the benzene rings of 1.2-bis(diphenylphosphino)ethane and the benzothiazole component of the metallated ligand in complex **1** (Fig. 1a) define the mutual anisotropic action of circular currents, which leads to the strong-field shift of the signals of H^4 and H^o atoms by 1.2 and 0.7 ppm (Table 3).

Magnetic equivalence of two donor atoms, C$^{1'}$ in the ligand *t*-BuNC and P$^{1''}$ in the ligand Edp, in the ^{13}C

Table 2. Bond length and bond angles of complexes **2** and **4**

d, Å	$[Ir(bt)_2(Edp)]PF_6 \cdot CH_3CN$	$[Ir(bt)_2(Dtc)]$
Ir–C(bt)	2.066(3), 2.063(3)	2.015(6)
Ir–N(bt)	2.093(3), 2.086(3)	2.099(5)
Ir–P(Edp)	2.408(1), 2.404(1)	–
Ir–S(Dtc)	–	1.737(8)
P–C(Ph)	1.832(6), 1.834(4) 1.829(4), 1.840(4)	–
P–CH_2	1.833(4), 1.836(4)	–
C–N(Dtc)	–	1.406(8)
φ, deg	$[Ir(bt)_2Edp]PF_6 \cdot CH_3CN$	$[Ir(bt)_2Dtc]$
N(bt)IrC(bt)	79.1(1)	79.3(1)
C(bt)IrC(bt)	85.7(2)	93.4(1)
C(bt)IrP(Edt)	96.2(1), 95.7(1)	–
C(bt)IrS(Dtc)	–	97.4(1)
P(Edt)IrP(Edt)	82.98(3)	–
S(Dtc)IrS (Dtc)	–	71.9(1)
N(bt)IrN(bt)	163.1(1)	167.2(2)

Table 3. Changes in chemical shifts ($\delta_{comp} - \delta_{b.\ ligand}$, ppm) of ligand atoms nearest to Ir(III) in complexes

Comp. no.	Atom	{Ir(bt)}						{Ir(tBuNC)$_2$}, {Ir(Edp)}, {Ir(Exn)}, {Ir(Dtc)}				
		1	3	4	1'	2'	3'	1"	2"	4"	*ipso*	*ortho*
1	^{1}H	–	–	0.7	–	–	–0.7	–	–	0.3	–	–
	^{13}C	14.6	0.5	–6.0	15.3	12.1	–0.5	–3.7	–	–0.9	–	–
2	^{1}H	–	–	–1.2	–	–	–1.3	–	1.2	–	–	–0.7
	^{13}C	13.6	2.2	–6.6	12.2	11.0	–1.2	–	0.5	–	–2.8	0.5
3	^{1}H	–	–	0.9	–	–	–1.0	–	–	–0.3	–	–
	^{13}C	12.3	–3.7	–7.9	18.0	12.0	–1.6	–	[a]	8.3	–	–
4	^{1}H	–	–	1.3	–	–	–0.9	–	–	–0.9	–	–
	^{13}C	12.0	–2.4	–8.4	21.4	12.1	–1.8	–	3.2	–6.4	–	–

[a] Low intensity of signal.

Table 4. Optical, IR, and electrochemical characteristics of complexes

Comp. no.	λ_{max}, nm ($\varepsilon\times10^3$ L mol^{-1} cm^{-1})		λ_{max}^{emis}, nm (τ, μs)	ν, cm^{-1}		E_p, V[a]	
	Intraligand	CTML		CN/CO	SCS	Ox	Red
1	267 (18.1), 313 (29.8), 325 sh (26)[b]	361 (15.7), 380 sh (12)[b]	508, 539, 595 sh (6)[b]	2199, 2170	–	1.42	–2.01[c], –2.29[c]
2	270 sh (18), 310 sh (17), 321(19.3)[b]	371 (7.66), 395 sh (5.5), 415 sh (1.7)[b]	506, 540, 585, 635 sh (14)[b]	–	–	1.11	–1.99[c], –2.25[c]
3	264 (34.1), 300 sh (31), 312 (36.8), 325 (35.3)[d]	362 (10.8), 395 (7.9), 433 (6.37), 465 sh (4.9)[d]	542, 587, 638 (6)[d]	1234	1023, 998, 715	0.65	–2.29, –2.47
4	270 sh (33), 314 (37.6), 330 sh (30)[d]	379 (7.83), 412 (6.74), 446(5.02)[d]	556, 600 sh, 675 sh (5)[d]	1488	1024, 997, 714	0.64	–2.25[c], –2.49

[a] $C_6H_5CH_3$–CH_3CN, 1 : 1. [b] CH_3CN. [c] $E_{1/2}$. [d] CH_2Cl_2.

and ^{31}P NMR spectra of complexes **1** and **2** confirms their *trans*-position in relation to the donor $C^{1'}$ atoms of cyclometallated ligands and the bidentate coordination of Edp in complex **2**. The increase in the electron density on $C^{1'}$ atoms, signals of which are shifted upfield by 3.7 ppm as a result of interaction with the metal (Table 3), is consistent with π-acceptor properties of the ligand *t*-BuNC.

The increase in the donor and the decrease in the acceptor properties of ligands in the sequence *t*-BuNC ~ Edp < Dtc^- ~ Exn^- lead to a downfield shift of the signals of the C^1 and $C^{1'}$ atoms nearest to the metal atom (Table 3), which reflects the increase and decrease in electron density on the benzothiazole and phenyl components of the cyclometallated ligand.

Thus, cyclometallated complexes **1**–**4** are in the form of the *cis*-C,C-isomers with octahedral structure disturbed along the axial axis. The variation of the donor-acceptor interaction between the metal and

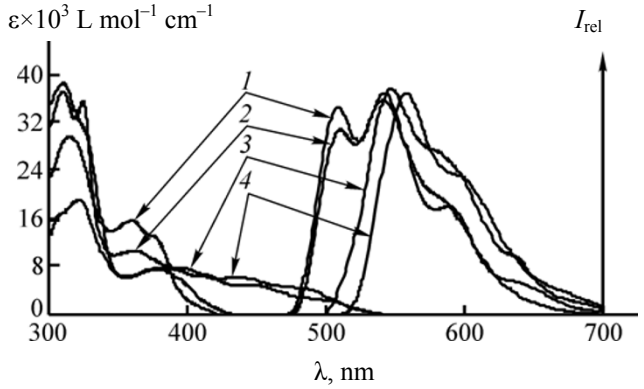

Fig. 2. Absorption and phosphorescence spectra of complexes (*1*) $[Ir(bt)(tBuNC)_2]PF_6$, (*2*) $[Ir(bt)_2Edp]PF_6$, (*3*) $[Ir(bt)_2Exn]$, (*4*) $[Ir(bt)_2Dtc]$.

t-BuNC, Edp, Dtc^-, and Exn^- ligands leads to the variation in the electron density on cyclometallated ligands.

Within the model of presumable localized nature of molecular orbitals [12], the electron absorption spectra of the complexes are characterized by two types of spin-allowed optical transitions typical for cyclometallated Ir(III) complexes with 2-phenylbenzotiazole [5–8, 13, 14]. Intensive ($\varepsilon \sim 10^4$ L mol^{-1} cm^{-1}) absorption bands resulted from the intraligand optical π–π* transitions, which are presumably localized on a cyclometallated ligand, are observed in the range of 250–350 nm (Fig. 2). More long-wave and less intensive ($\varepsilon \sim 10^3$ L mol^{-1} cm^{-1}) absorption bands are associated with the charge transfer metal-cyclometallated ligand (CTML) optical transitions d_π–π* (bt). Whereas the blue shift of intraligand absorption bands of complexes **1**–**4** is less than 400 cm^{-1}, the replacement of π-donor Dtc^- and Exn^- ligands by π-acceptor *t*-BuNC and Edp ligands leads to the blue shift of CTML bands by ~3800 cm^{-1} (Fig. 2).

On assumption that Koopans theorem [15] is valid, a similar nature of HOMO and LUMO of complexes involved in photo- and electro-stimulated processes should be expected. The oxidation and reduction voltammograms of the complexes are characterized (Fig. 3) by one-electron waves of electron transfer with the participation of Ir(III) d_π-orbitals presumably localized on the $\{Ir(bt)_2\}$ metal complex fragment and π*-orbitals of the cyclometallated ligand.

$$[Ir^{(III)}(bt)_2(L,L)]^Z - e^- = [Ir^{IV}(bt)_2(L,L)]^{Z+1},$$

$$[Ir(bt)_2(L,L)]^Z + e^- = [Ir(bt)(bt^-)(L,L]^{Z-1},$$

$$[Ir(bt)(bt^-)(L,L)]^{Z+1} + e^- = [Ir(bt^-)_2(L,L)]^{Z-2}.$$

The replacement of the chelating π-donor ligands Dtc^- and Exn^- by the π-acceptor *t*-BuNC and Edp ligands leads to the anodic shift of the oxidation and reduction potentials of the complexes by 0.77–0.46 and ~0.27 V (Table 4). This is consistent with the change in the electron density of $C^{1'}$ and C^1 atoms of the metallated phenyl and benzothiazole components of the cyclometallated ligands in complexes **1** and **2** (Table 3) and with the elongation of the Ir–C(bt) bond in complex **2** (Table 2). The increase in the difference of oxidation and reduction potentials of complexes **1** and **2** in relation to complexes **3** and **4** agrees with the blue shift of their CTML absorption bands.

Photoexcitation of solutions of the complexes in the region of intraligand (IL) and CTML absorption bands results in vibration-structured phosphorescence in the visible spectral caused by the spin-forbidden radiative process of excitation energy degradation from the lowest in energy mixed IL/CTML electron-excited state. The blue shift by ~1800 cm^{-1} and better resolved vibration structure of phosphorescence spectrum with vibration frequency of ~1300 cm^{-1} close to the frequency of the C=N bond vibration in metallated 2-phenylbenzothiazole [13] point to a decrease in the CTML admixture to intraligand bands in complexes **1** and **2** containing π-acceptor ligands *t*-BuNC and Edp.

The results of the work show that weakening donor and strengthening acceptor properties of ligands lead to the blue shift in the absorption and phosphorescence spectra, and to the anodic shift of oxidation and reduction potentials of Ir(III) cyclometallated complexes that allows modifying optical and electrochemical characteristics of the phosphors.

EXPERIMENTAL

X-ray diffraction studies were carried out at 100 K on Agilent Technologies Excalibur Eos and SuperNova diffractometers equipped with flat detectors of reflected X-rays CCD, MoK_α (λ = 0.71073 Å) and CuK_α (λ =1.54184 Å) radiations, respectively, at the Research Center for X-ray Diffraction Studies of St. Petersburg State University. Unit cell parameters were refined by the least squares method. The structures were solved by the direct method and refined by the program SHELX [16] of the program complex OLEX2 [17] by the full-matrix least squares method in the anisotropic approximation. A correction for absorption was introduced in the program complex CrysAlisPro [18]. Hydrogen atoms were included in the refinement with fixed position and temperature parameters. Crystallographic data for complexes **2** and **4** were deposited in Cambridge Crystallographic Data Center [CCDC 1475139 (**2**), 1058768 (**4**)].

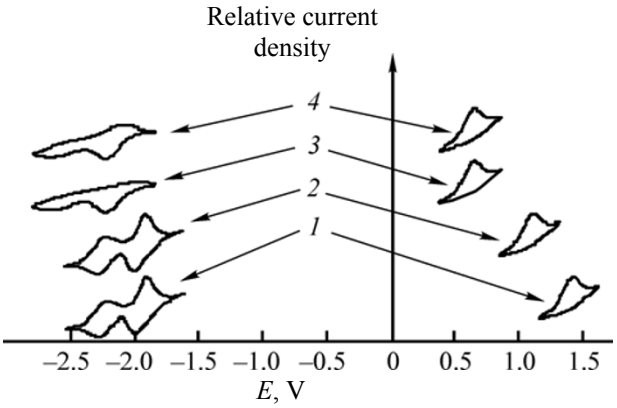

Fig. 3. Oxidation and reduction voltammograms of complexes (*1*) $[Ir(bt)(tBuNC)_2]PF_6$, (*2*) $[Ir(bt)_2Edp]PF_6$, (*3*) $[Ir(bt)_2Exn]$, (*4*) $[Ir(bt)_2Dtc]$.

The ^1H, ^{13}C, and ^{31}P NMR spectra of the complexes in $CDCl_3$ and $(CD_3)_2SO$ and the IR spectra in KBr tablets were taken on JNM-ECX400A and IR Prestige 21 spectrometers of Common use center of the chemical faculty of the Russian State Pedagogical University. The electronic absorption and emission spectra were recorded in CH_2Cl_2 and CH_3CN on an SF-2000 spectrophotometer and a Fljuorat-2 Panorama spectrofluorimeter.

The voltammograms were obtained on an IPC-PRO installation in a cell with separated spaces of main (GC), auxiliary (Pt), and reference (Ag) electrodes in the presence of a 0.1 M $[N(C_4H_9)_4]PF_6$ solution in the mixture $C_6H_5CH_3$: CH_3CN, 1 : 1. Potentials are given in relation to the ferrocenium/ferrocene redox system.

Complexes **1**–**4** were obtained with the yield of ~50% by the procedures [5, 7].

Bis[(2-phenyl-3-ido)benzothiazole)]di(*tert*-butylisocyanide)iridium(III) hexafluorophosphate (1). ^1H NMR spectrum [$(CD_3)_2SO$], δ, ppm (*J*, Hz): {Ir $(bt)_2$}, 8.84 ($2H^4$, $^3J_{HH}$ = 8.3), 8.80 ($2H^7$, $^3J_{HH}$ = 8.0) 8.40 d ($2H^{6'}$, $^3J_{HH}$ = 7.2), 8.39 d.d.d ($2H^5$, $^3J_{HH}$ = 8.4 7.4, $^4J_{HH}$ = 1.1), 8.26 t.d ($2H^6$, $^3J_{HH}$ = 8.0, $^4J_{HH}$ = 0.8) 7.61 t.d ($2H^{5'}$, $^3J_{HH}$ = 7.6, $^4J_{HH}$ = 0.9) 7.46 t.d ($2H^{4'}$, $^3J_{HH}$ = 7.6, $^4J_{HH}$ = 1.1), 6.84 d ($2H^{3'}$, $^3J_{HH}$ = 7.6); {Ir(BuNC)}, 1.83 s (18 $H^{4'}$). ^{13}C NMR spectrum [$(CD_3)_2SO$)], δ_C, ppm; {Ir$(bt)_2$}, 182.6 ($2C^1$), 154.5 ($2C^3$), 150.3 ($2C^{3'}$), 141.0 ($2C^{2'}$), 132.8 ($2C^{6'}$), 132.3 ($2C^8$), 130.8 ($2C^5$), 127.0

($2C^{3'}$), 125.7 ($2C^{6}$), 125.1 ($2C^{6}$), 124.9 ($2C^{4}$), 118.2 ($2C^{4'}$); {Ir(BuNC)}, 150.3 ($2C^{1''}$), 37.3 ($2C^{3'}$), 29.9 ($6C^{4'}$).

Bis[(2-phenyl-3-ido)benzothiazole)][1.2-bis(diphenylphosphino)ethane]iridium(III) hexafluorophosphate (2) ^{1}H NMR spectrum [$(CD_3)_2SO$], δ, ppm (*J*, Hz): {$Ir(bt)_2$}, 7.95 d ($2H^{6'}$,$^3J_{HH}$ = 7.6), 7.85 d.d ($2H^{7}$, $^3J_{HH}$ = 8.1, $^4J_{HH}$ = 1.0), 7.43 t ($2H^{5'}$, $^3J_{HH}$ = 7.3), 7.22 t.d ($2H^{6}$, $^3J_{HH}$ = 8.0, $^4J_{HH}$ = 0.8), 7.17 t.d ($2H^{5}$, $^3J_{HH}$ = 7.8, $^4J_{HH}$ = 0.9), 7.02 t ($2H^{4'}$,$^3J_{HH}$ = 7.6), 6.80 d ($2H^{4}$, $^3J_{HH}$ = 8.4), 6.15 d ($2H^{3'}$, $^3J_{HH}$ = 7.8); {Ir(Edp)}, 7.38–7.35 m ($6H^{Ph}$), 7.29-7.25 m ($4H^{Ph}$), 6.66–6.62 m ($10H^{Ph}$), 3.24 d ($2H^{2'}$, $^3J_{HH}$ = 8.4), 2.55 m ($2H^{3'}$). ^{13}C NMR spectrum [$(CD_3)_2SO$], δ_C, ppm: {$Ir(bt)_2$}, 181.6 ($2C^{1}$), 156.2 ($2C^{3}$), 147.2 ($2C^{1'}$), 139.9 ($2C^{2'}$), 132.6 ($2C^{8}$), 132.6 ($2C^{6'}$), 130.8 ($2C^{5'}$), 126.3 ($2C^{3'}$), 125.8 ($2C^{5}$), 125.4 ($4C^{6}$), 124.3 ($2C^{4}$), 123.7 ($2C^{7}$), 120.6 ($2C^{4'}$); {Ir(Edp)}, 135.8 ($2C^{Ph}$, J_{CP} 44.0), 132.4 ($4C^{Ph}$), 128.7 ($2C^{Ph}$), 128.3 (4^{Ph}), 24.5 ($2C^{,3''}$). ^{31}P NMR spectrum [$(CD_3)_2SO$], δ_P, ppm (*J*, Hz): –143.8 (J_{PF} = 711.0), 4.89 d.d (J_{PC} = 249.0, $^4J_{PP}$ = 18.0).

Bis[(2-phenyl-3-ido)benzothiazole](ethylxanthogenato)iridium(III) (3). 8.96 m ($2H^{4}$), 7.93 m ^{1}H NMR spectrum ($CDCl_3$), δ, ppm (*J*, Hz): {$Ir(bt)_2$}, ($2H^{7}$), 7.68 d.d ($2H^{6'}$, $^3J_{HH}$ = 7.7, $^4J_{HH}$ = 1.0), 7.47, d.d.d ($2H^{6}$, $^3J_{HH}$ = 7.4, 7.2, $^4J_{HH}$ = 1.4), 7.51 d.d.d ($2H^{5}$, $^3J_{HH}$ = 7.8, 7.2, $^4J_{HH}$ = 1.5), 6.88 t.d ($2H^{5'}$, $^3J_{HH}$ = 7.6, $^4J_{HH}$ = 1.0), 6.68 d.d.d ($2H^{4'}$, $^3J_{HH}$ = 7.7, 7.4, $^4J_{HH}$ = 1.4) 6.53 d ($2H^{3'}$, $^3J_{HH}$ = 7.8); {Ir(Exn)}, 4.56 q ($H^{4'}$, $^3J_{HH}$ = 7.1), 4.44 q ($H^{4'}$, $^3J_{HH}$ = 7.1), 1.35 t ($3H^{5''}$, $^3J_{HH}$ = 7.1). ^{13}C NMR spectrum ($CDCl_3$), δ_C, ppm: {$Ir(bt)_2$}, 180.3 ($2C^{1}$), 153.0 ($2C^{1'}$), 150.8 ($2C^{3}$), 140.9 ($2C^{2'}$), 133.9 ($2C^{6'}$) 131.6 ($2C^{8}$), 129.6 ($2C^{5'}$), 126.6 ($2C^{5}$), 125.9 ($2C^{3'}$), 124.9 ($2C^{6}$), 123.0 ($2C^{4}$), 122.2 ($2C^{7}$), 121.0 ($2C^{4'}$); {Ir(Exn)}, 66.6 ($C^{4''}$), 13.8. ($C^{5''}$).

Bis[(2-phenyl-3-ido)benzothiazole](diethyldithiocarbamato)iridium(III) (4). ^{1}H NMR spectrum ($CDCl_3$), δ, ppm (*J*, Hz): {$Ir(bt)_2$}, 9.43 d ($2H^{4}$, $^3J_{HH}$ = 7.9), 7.91 d ($2H^{7}$, $^3J_{HH}$ = 7.7), 7.66 d ($2H^{6'}$, $^3J_{HH}$ = 7.5), 7.50 d.d ($2H^{5}$, $^3J_{HH}$ = 8.1, 7.1), 7.45 d.d ($2H^{6}$, $^3J_{HH}$ = 8.0, 7.2), 6.83 d.d ($2H^{5'}$, $^3J_{HH}$ = 7.5, 7.2), 6.64 d.d ($2H^{4'}$, $^3J_{HH}$ = 7.6, 7.1), 6.58 d ($2H^{3'}$,$^3J_{HH}$ = 7.6); {Ir(Dtc)}, 3.96 q ($2H^{4''}$, $^3J_{HH}$ = 6.9), 3.18 q ($2H^{6''}$, $^3J_{HH}$ = 6.9), 1.14 q ($6H^{5'',7''}$, $^3J_{HH}$ = 6.9). ^{13}C NMR spectrum ($CDCl_3$), δ_C, ppm: {$Ir(bt)_2$}, 180.0 ($2C^{1}$), 156.4 ($2C^{1'}$), 151.6 ($2C^{3}$), 141.0 ($2C^{2'}$), 133.7 ($2C^{6'}$), 132.1 ($2C^{8}$) 130.2 ($2C^{5'}$), 127.1 ($2C^{5}$), 125.7 ($2C^{3'}$), 125.3 ($2C^{6}$), 123.0 ($2C^{4}$), 122.5 ($4C^{4,7}$), 121.6 ($2C^{4'}$); {Ir(Dtc)}, 209.9 ($C^{2''}$), 43.2 ($2C^{4'',6''}$), 12.4 ($2C^{5'',7''}$).

REFERENCES

1. Chi, Y. and Chou, P.T., *Chem. Soc. Rev.*, 2010, vol. 39, no. 3, p. 638. doi 10.1039/B916237B
2. Kubas G.J., *J. Organomet. Chem.*, 2009, vol. 694, no. 17, p. 2648. doi 10.1016/j.jorganchem.2009.05.027
3. Leung, C.-H., Zhong, H.-J., Chan, D.S-H., and Ma, D.-L., *Coord. Chem. Rev.*, 2013, vol. 257, nos. 11–12, p. 1764. doi 10.1016/j.ccr.2013.01.034
4. Zhao, Q, Li, F., and Huang, C., *Chem. Soc. Rev.*, 2010, vol. 39, no. 8, p. 3007. doi 10.1039/B915340C
5. Katlenok, E.A., Zolotarev, A.A., and Balashev, K.P., *Russ. J. Coord. Chem.*, 2015, vol. 41, no. 1, p. 37. doi 10.7868/S0132344X15010041
6. Katlenok, E.A., Zolotarev, A.A., Ivanov, A.Yu., Smirnov, S.N., Baichurin, R.I., and Balashev, K.P., *Russ. J. Gen. Chem.*, 2015, vol. 85, no. 11, p. 2634. doi 10.1134/S1070363215110213
7. Yun, S-J., Song, Y.-K., Kim, M., Shin, J, Jin, S.-H., Kang, S.K., and Kim, Y.-I., *Bull. Korean Chem. Soc.*, 2014, vol. 35, no. 11, p. 3199. doi 10.512/bkcs.2014.35.11.3199
8. Radwan, Y.K. Maity, A., and Teets, T.S., *Inorg. Chem.*, 2015, vol. 54, no. 14, p. 1722. doi 10.1021/acs.inorgchem. 5b01401
9. Fornies, J., Sicilia, V., Casas, J.M., Martin, A., Lopez, J.A., Larraz, C., Borja, P., and Ovejero, C., *Dalton Trans.*, 2011, vol. 40, no. 12, p. 2898. doi 10.1039/C0DT01451F
10. Nakamoto, K., *Infrared and Raman Spectra of Inorganic and Coordination Compounds*, New York: John Wiley, 1986.
11. Bonati, F. and Ugo, R., *J. Organomet. Chem.*, 1967, vol. 10, no. 2, p. 257. doi 10.1016/S0022-328X(0000)93085-7
12. DeArmond, K., Hanck, K.W., and Wertz, D.W., *Coord. Chem. Rev.*, 1985, vol. 64, p. 65. doi 10.1016/0010-8545(85)-800424
13. Katlenok, E.A. and Balashev, K.P., *Optics and Spectr.*, 2013, vol. 114, no. 5, p. 756. doi 10.7868/S0030403413040107
14. Lamansky, F., Djurovich, P., Murphy, D., Abdel-Razzaq, F., Le, H.-E., Adachi, C., Burrows, P.E., Forrest, S.R., and Thomson, M.E., *J. Am. Chem. Soc.,* 2001, no. 18, p. 4304. doi 10.1021/ja003693s
15. Koopmans, T., *Phisics,* 1933, vol. 1, no. 1, p. 104.
16. Sheldrick, G.M., *Acta Crystallogr. (A)*, 2008, vol. 64, no. 1, p. 112. doi 10.1107/S0108767307043930
17. Dolomanov, O.V., Bourhis, L.J., Gildea, R.J., Howard, J.A.K., and Puschmann, H., *J. Appl. Crystallogr.*, 2009, vol. 42, no. 2, p. 339. doi 10.1107/S0021889808042726
18. *CrysAlisPro,* Agilent Technologies, Version 1.171.36.20 (release 6/27/2012).